Quantum Chemical Modeling of Through-Hydrogen Bond Spin – Spin Coupling in Amides and Ubiquitin**

Alessandro Bagno*[a]

Abstract: Through-hydrogen bond spin – spin coupling has been investigated computationally in the formamide dimer and in fragments of the protein ubiquitin. The Fermi-contact term was calculated by finite perturbation theory with the B3LYP DFT method with several basis sets. The distance and angular dependence of the $^3J_{N,C'}$ coupling constant (N–H···O=C) in the hydrogen-bonded formamide dimer was firstly examined for a wide range of mutual arrangements, also in relation to the stability of the dimer. The magnitude of $^3J_{N,C'}$ is relatively insensitive to the dihedral angle between the two amide planes, whereas values between 1 – 2 Hz are calculated for a variety of arrangements, including non-linear hydrogen bonds, in agreement with the shape of some occupied, low-lying molecular orbitals which connect donor and acceptor. Then, fragments of the ubiquitin protein (for which such coupling constants are experimentally available) were generated by removing from the experimental structure all amino acids except those involved in hydrogen bonding, and coupling constants were calculated for such fragments. Although calculated $^3J_{N,C'}$ values are sometimes overestimated, they generally correlate with the corresponding experimental values.

Keywords: ab initio calculations · amides · NMR spectroscopy · peptides · spin – spin coupling

Introduction

The secondary structure of biomolecules is largely dictated by the formation of specific hydrogen bonds (HB) between, for example, amino acid or nucleic acid residues; in peptides, the amino acids involved may be quite far apart in the primary structure, that is separated by a large number of covalent bonds. Normally, the existence of a specific HB is inferred indirectly from the spatial proximity of the donor and acceptor moieties, as probed by X-ray crystallography or NMR measurements.[1] Hence, there is a long-standing need for a method capable of directly probing the existence of a HB. Very recently, scalar coupling between nuclei separated by a HB have been successfully probed by NMR methods. Thus, the observed ^{1}H – ^{113}Cd coupling in rubredoxin was found to be mediated by a NH···S(Cys) HB,[2] and ^{15}N–H··· ^{15}N coupling between base pairs in DNA and RNA was demonstrated by means of various 2D-NMR techniques.[3–5] Likewise, ^{13}C – ^{15}N couplings in proteins ($^3J_{N,C'}$, ^{15}N–H··· O=^{13}C),[6–8] ^{15}N – ^{19}F couplings in a collidine/HF complex[9] and ^{19}F – ^{1}H couplings in $(HF)_n$ clusters[10] were observed. Whereas internucleotide couplings ($^2J_{N,N}$) are about 7 Hz, known interresidue couplings in proteins never exceed 1 Hz; both require special NMR techniques, as well as isotopic labeling, to be detected.

Of course, the determination and the understanding of such couplings bear a considerable interest from both a fundamental and practical viewpoint, since they help elucidating the nature of the hydrogen bond, and also provide a very valuable tool for structure determination in solution, since this interaction unambiguously singles out the atoms involved in the HB. Hence the importance of predicting these couplings, with the aim of understanding their origin and their structural dependence. Given our current interest in NMR probes for solvation and hydrogen bonding,[11, 12] we have undertaken a theoretical study of $^3J_{N,C'}$ couplings in a model system (formamide dimer), and a protein in its experimental conformation (ubiquitin) for which such couplings are experimentally available.[6]

Results

An excellent review on the calculation of scalar couplings by ab initio quantum chemical methods has been recently published.[13] For light atoms, the major contribution to spin – spin coupling is the Fermi-contact (FC) interaction.

[a] Dr. A. Bagno
Centro CNR Meccanismi Reazioni Organiche
Dipartimento di Chimica Organica, Università di Padova
via Marzolo 1, 35131 Padova (Italy)
Fax: (+39) 0498275239
E-mail: alex@chor.unipd.it

[**] Supporting information for this contribution is available on the WWW under http://www.wiley-vch.de/home/chemistry/

  0947-6539/00/0616-2925 $ 17.50+.50/0

The latter can be reliably calculated by finite perturbation theory (FPT), as demonstrated for boranes[14] and DNA base pairs.[5] Although accurate calculations have shown that for the water dimer the paramagnetic spin–orbit term is not negligible,[15] recent calculations[16] on the *N*-methylacetamide dimer have emphasized that the FC term accounts for 96% of the total magnitude of $^3J_{N,C'}$. The effect of electron correlation, and in particular of density functional theory, on the calculation of coupling constants was emphasized.[5, 9, 13–16] Therefore, the calculation of the FC term at a correlated level of theory seems to be adequate for this purpose.

***J* coupling in the formamide dimer**: The scalar coupling between amino acids was firstly investigated in the formamide dimer model system. Although accurate calculations have been run on a similar system (*N*-methylacetamide dimer),[16] only a limited series of spatial arrangements of the two molecules was considered. In particular, the possible effect of the non-coplanarity of the two amide systems (a common arrangement in proteins), and the relationship between stability of the HB and the magnitude of coupling, were not considered. Moreover, the behavior of this system was taken to be a model of through-HB couplings in proteins, even though the environment provided by the protein interior is expected to play a role.

Hence, we determined the energy and spin–spin coupling constants for the dimer of formamide in a variety of arrangements, as depicted in Scheme 1. A similar study, dealing with

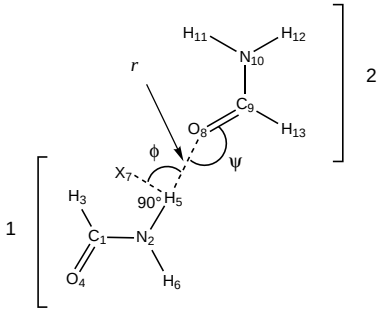

Scheme 1. Geometry and numbering system of the formamide dimer. X7 is a dummy atom (located at an arbitrary distance from H5 and forming an angle of 90° with N2), needed for the optimization in internal coordinates to work even with a linear hydrogen bond ($\phi = 90°$). The system represented is the planar one, i.e., with d (X7-H5-O8-C9 dihedral) $= 0°$; the H5-X7 vector lies in the N2-H5-O8 plane.

the interaction energy of formamide and *N*-methylacetamide, emphasized that the dependence of the HB binding energy on torsion angles is stronger than in formamide, owing to the larger steric bulk in the former.[17]

All coupling constants are calculated for the ^{1}H, ^{15}N, ^{17}O, and ^{13}C nuclei. For brevity, herein we present these results in a graphical form only. The full data set (internal coordinate system, energies and coupling constants as a function of r, ψ, ϕ, and d) is contained in the Supporting Information. All calculated $^3J_{N,C'}$ values are negative,[8, 16] and are compared with experimental data as absolute values.

In the following calculations, the internal coordinates of each individual $HCONH_2$ molecule were kept fixed at the values resulting from a preliminary unconstrained B3LYP/6-311G(d,p) optimization.

Firstly, the potential-energy (PES) and coupling surface was scanned as a function of a) r (H5–O8 distance) between 1.7 and 2.1 Å in 0.1 Å steps; b) ψ (H5-O8-C9 angle) between 135 and 180° in 5° steps; c) d (X7-H5-O8-C9 dihedral) between 0 and 180° in 5° steps. The angle ϕ (X7-H5-O8) was kept fixed at the value of 79.6°, that is the value resulting from the preliminary optimization (N2-H5-O8 angle 169.6°). In this way, the dependence on the torsion angle between the two amide system planes could be investigated. Since it became apparent that the torsion angle d has little influence on the magnitude of the coupling constants (see below), a new scan was run assuming a planar system ($d = 0°$) and examining only the influence of r, ψ (varied as before), and ϕ (varied between 30 and 150° in 30° steps). Energy and coupling constant calculations were run with the RB3LYP or UB3LYP method, respectively, with the 6-31G(d,p) basis set. The binding energies were calculated as $E_b = 2E(HCONH_2) - E(\text{dimer})$. Even though the scope of this work requires only relative energies, it is useful to obtain the basis set superposition error (BSSE) in the calculated E_b values. To this effect, we also carried out counterpoise calculations[18] on a sample of the PES ($\phi = 90°$, $\psi = 135°$, $d = 60$, $r = 1.7–2.1$ Å). Whereas the uncorrected binding energies increase from -5.4 to -7.1 kcal mol^{-1} upon increasing r, the corresponding corrected values lie between -3.7 and -5.8 kcal mol^{-1}, with a BSSE of ca. 1.5 kcal mol^{-1} not much dependent on r (at least in the narrow range investigated). Hence, although HB energies should be shifted accordingly, the BSSE will not affect the general features of the PES.

The potential-energy and coupling surfaces of the second scan ($d = 0°$) are collected in Figure 1 and Figure 2 as contour maps, blue and red regions representing stabilizing/weak coupling and destabilizing/strong coupling, respectively.

The energy and coupling information is shown together in Figure 3, where the coupling surfaces (excluding that with $\phi = 30°$, which is largely repulsive) are color-coded according to the binding energy. Thus, blue and red regions of the surface represent stabilizing and destabilizing interactions, respectively, for a given magnitude of the coupling constant. From that Figure one can appreciate the bell-shaped dependence of J on the angle ψ, with a maximum at about 150°, and the smooth decrease with increasing r. Given the flexibility of this system, and hence the dependence of J on several variables, it is not possible to reduce it to a simple functional form like the Karplus equation. However, the families of curves obtained can be fit to second grade polynomials against r for all ψ values (and vice versa), thus obtaining empirical relationships which allow the estimation of J as a function of the relevant geometrical parameters. A sample of such polynomial coefficients is presented in Tables 1 and 2 for the case $\phi = 90°$, $d = 0°$ in the form $J(\psi)_r = a_0 + a_1 \sin\psi + a_2 \sin^2\psi$ ($r = 1.7–2.1$ Å) and $J(r)_\psi = b_0 + b_1 r + b_2 r^2$ ($\psi = 135–180°$).

We finally note that the coupling between N2 and other nuclei in the acceptor formamide molecule beyond C8 (N10, H11, H12) is negligible (see below for the through-HB coupling to O).

  0947-6539/00/0616-2926 $ 17.50+.50/0 *Chem. Eur. J.* **2000**, *6*, No. 16

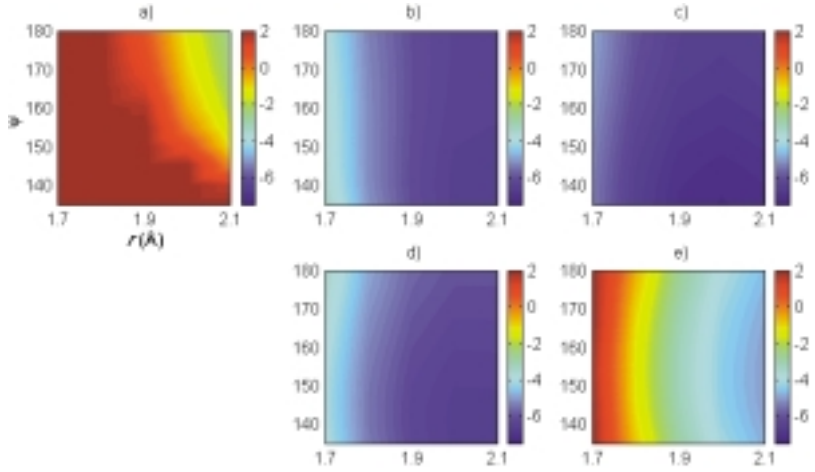

Figure 1. Potential-energy surfaces [kcal mol^{-1}] of the planar formamide dimer ($d = 0°$) as a function of r [Å] and ψ for $\phi = 30 - 150°$ (RB3LYP/6-31G(d,p)). a) – e): $\phi = 30, 60, 90, 120, 150°$. For clarity, axis labels (the same for all plots) are given only on plot a). Red and blue correspond to stabilizing and destabilizing regions, respectively.

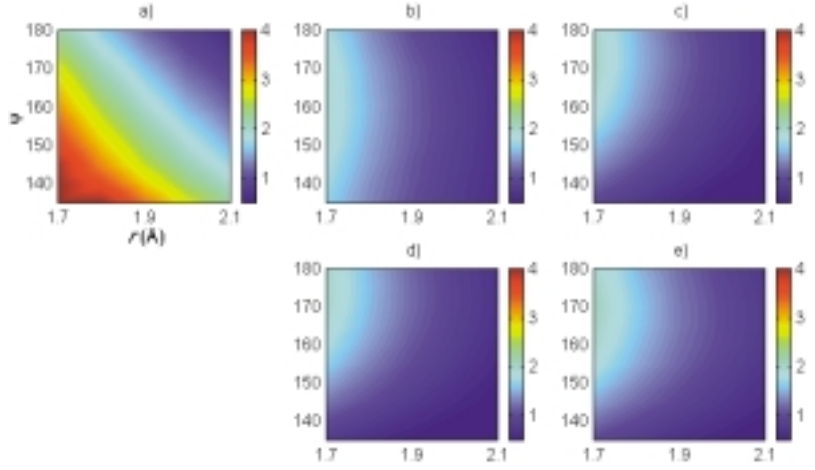

Figure 2. Coupling surfaces ($^3J_{N,C'}$/Hz) of the planar formamide dimer ($d = 0°$) as a function of r [Å] and ψ for $\phi = 30 - 150°$ (UB3LYP/6-31G(d,p)). Red and blue correspond to strong and weak coupling, respectively. See caption to Figure 1.

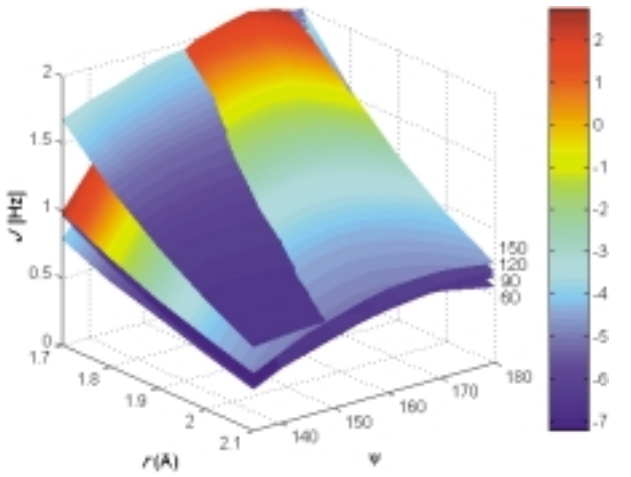

Figure 3. Coupling surfaces ($^3J_{N,C'}$/Hz) of the formamide dimer for $d = 0°$ and $\phi = 60 - 150°$ as a function of r [Å] and ψ (UB3LYP/6-31G(d,p)), color-coded with interaction energy (kcal mol^{-1}) according to the color bar at the right. The foremost (blue) surface is for $\phi = 60°$.

Some molecular orbitals (HOMO-10, HOMO-11 and HOMO-13) of the formamide dimer with substantial density in the HB region are depicted in Figure 4. Since the system has 24 occupied MOs, the three above ones are fully occupied and rather low-lying in energy (#14, #13, and #11, respectively); they also have approximately σ symmetry. On the other hand, no MO having π symmetry connects the two interacting molecules.

***J* coupling in ubiquitin**: Couplings in ubiquitin were firstly investigated by examining some weak intraresidue coupling constants in the V17 ($^2J_{N,C'}$), D32 and N60 ($^3J_{N,C^\gamma}$) residues. The input geometry was obtained from the X-ray structure of ubiquitin[19] by removing all amino acids except the one of interest, and replacing the two adjacent ones by -$COCH_3$ groups, thereby retaining the original structure and conformation in the fragment studied. J values were calculated at the UHF or UB3LYP/6-31G(d,p) levels and are reported in Table 3; as will be detailed later, this basis set is an optimum trade for accuracy versus cost. Although HF values are overestimated (by a factor of ca. two), the correlation with experimental values is very good. DFT values are much closer to experiment, but the correlation is slightly worse (see Figure 5).

Input geometries for interresidue couplings were obtained in a similar way, that is all amino acids were removed except the two H-bonded ones, and all four adjacent residues replaced by -$COCH_3$ groups. In this way, not only the original conformation is retained, but the effect of the environment is partly introduced, which was suggested to be an important

Table 1. Polynomial coefficients for the dependence of $^3J_{N,C'}$ [Hz] on the angle ψ for various hydrogen-bonding distances r [Å].[a]

r	a_0	a_1	a_2
1.7	1.98	0.8	– 3.2
1.8	1.48	0.6	– 2.3
1.9	1.14	0.4	– 1.7
2.0	0.82	0.5	– 1.6
2.1	0.59	0.5	– 1.2

[a] $J(\psi) = a_0 + a_1 \sin\psi + a_2 \sin^2\psi$; $\phi = 90°$. See text and Scheme 1 for symbol definitions.

  0947-6539/00/0616-2927 $ 17.50+.50/0

Table 2. Polynomial coefficients for the dependence of $^3J_{N,C'}$ [Hz] on the hydrogen-bonding distance r [Å] for various ψ angles.[a]

ψ	b_0	b_1	b_2
135	9.2	−7.2	1.4
140	14.8	−12.9	2.9
145	18.1	−15.9	3.6
150	18.9	−16.3	3.6
155	22.2	−19.3	4.3
160	22.6	−19.5	4.3
165	25.8	−22.5	5.0
170	22.7	−19.5	4.3
175	18.0	−14.3	2.9
180	25.8	−22.5	5.0

[a] $J(r)=b_0+b_1r+b_2r^2$; $\phi=90°$. See text and Scheme 1 for symbol definitions.

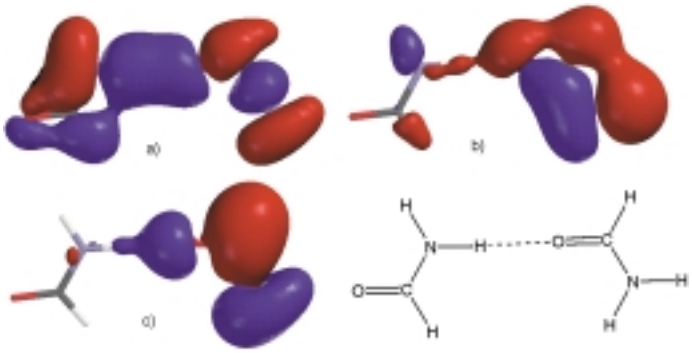

Figure 4. Three occupied molecular orbitals of the formamide dimer (RHF/6-31G(d,p)): a) HOMO-10 (MO #14); b) HOMO-11 (MO #13); c) HOMO-13 (MO #11).

Table 3. Intraresidue scalar couplings [Hz] in ubiquitin.[a]

Residue	Type	Exptl.	Calcd (HF)	Calcd (DFT)
V17	$^2J_{N,C'}$	0.50	1.1	−0.3
D32	$^3J_{N,C^\gamma}$	1.32	−3.0	−2.4
N60	$^3J_{N,C^\gamma}$	1.28	−2.8	−1.9

[a] Geometries from ref. [19], experimental coupling constants [Hz] from ref. [7]. Calculated values at the UHF or UB3LYP/6-31G(d,p) level.

factor.[16] The performance of some method/basis set combinations (which can be practical for systems of this size) was tested on the E64−Q2 fragment (Table 4).

The DFT method leads to markedly lower values of $^1J_{N,H}$ than with HF, but the interresidue couplings $^3J_{N,C'}$ are essentially converged to −1.0 (HF) or −1.2 Hz (DFT) regardless of whether the 6-31G or 6-311G basis (augmented in various ways) is used. The values of $^2J_{N,O}$ (N−H···O) are essentially converged to 7.1–7.2 Hz with all methods except UB3LYP/6-311G(d,p), which yields a significantly smaller value (6.3 Hz). However, with regard to the $^3J_{N,C'}$ couplings we can conclude that there is no significant advantage in using the larger

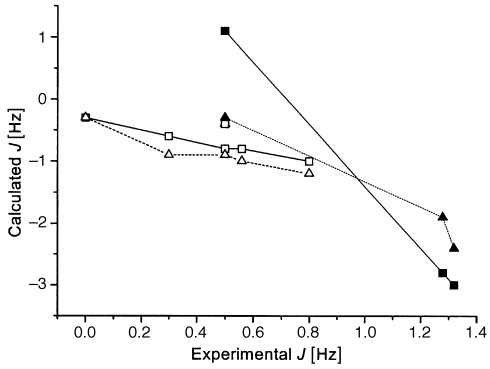

Figure 5. Calculated and experimental couplings [Hz] in ubiquitin fragments at the UHF or UB3LYP/6-31G(d,p) level. Experimental data are reported as absolute values. Intraresidue couplings (see text): HF (filled squares, solid line), DFT (filled triangles, dotted line). Interresidue couplings, $^3J_{N,C'}$: HF (open squares, solid line); B3LYP (open triangles, dotted line). The unavailable experimental value for K33−K29 has been arbitrarily set to zero. The data points for K27−I23 are not connected with the respective lines.

6-311G(d,p) basis. This is an important issue, since modeling a more extended peptide portion may be feasible without prohibitive computational costs.

In view of the expected sensitivity of the FC term to electron correlation effects,[15, 16] we ran all further calculations at the UB3LYP/6-31G(d,p) level.

The geometry of several HBs for which experimental interresidue couplings were available are collected in Table 5, and plotted against experimental data in Figure 5. Notably, K33-K29 coupling was not observed (implying a value <0.25 Hz[7]).

Discussion

Formamide dimer: The PES of the first scan are remarkably similar for all d values (see also[17]), maximum stabilization ($E_b \approx -7$ kcal mol^{-1}) being reached at $r \approx 2.0$ Å and $\psi = 135-140°$; the least stabilizing region lies at $r = 1.70-1.75$ Å, with a relatively flat region between 1.8–2.0 Å for nearly every value of ψ. The values of $^3J_{N,C'}$ (roughly between 0.5 and 1.9 Hz) decrease smoothly with increasing r, the slope being larger for lower ψ values. Given the strong dependence on r, the strongest coupling are expected for the least stable arrangements ($r = 1.70-1.75$ Å, $\psi = 160-180°$).

The potential-energy and coupling surfaces of the second scan ($d = 0°$) are collected in Figure 1 and Figure 2. They are

Table 4. Method and basis set effects on the calculated values of $J_{^{15}N-X}$ (X = ^{1}H, ^{17}O or ^{13}C) [Hz] in the E64−Q2 ubiquitin fragment.

Donor/Acceptor[a]	UHF			UB3LYP			Exptl.
	6-31G(d)	6-31G(d,p)	6-311G(d,p)	6-31G(d)	6-31G(d,p)	6-311G(d,p)	
E64^{H}N-Q2C′							
$^1J_{N,H}$[b]	−95.8	−92.2	−107.4	−78.1	−74.7	−87.1	
$^2J_{N,O}$[c]	7.1	7.1	7.2	7.1	7.1	6.3	
$^3J_{N,C'}$[d]	−1.0	−1.0	−1.1	−1.2	−1.2	−1.1	0.8

[a] According to this notation (after ref. [7]), E64 is the N−H donor and Q2 the carbonyl acceptor. [b] $^1J_{N,H}$ in the donor. [c] $^2J_{N,O}$ in N−H···O. [d] $^3J_{N,C'}$ in N−H···O=C.

0947-6539/00/0616-2928 $ 17.50+.50/0 *Chem. Eur. J.* **2000**, *6*, No. 16

Table 5. Geometry of hydrogen bonds, experimental and calculated scalar couplings $J_{^{15}N-X}$ (X = ^{1}H, ^{17}O or ^{13}C) [Hz] in ubiquitin fragments.[a]

Donor/Acceptor	r[b]	NHO angle	HOC angle	Torsion angle[c]	Secondary structure	HF	DFT	Exptl.[d]
E64^{H}N–Q2C′	1.84	155.3	174.0	59	random coil			
$^{1}J_{N,H}$						– 92.2	– 74.7	
$^{2}J_{N,O}$						7.1	7.1	
$^{3}J_{N,C'}$						– 1.0	– 1.2	0.8
R72^{H}N–Q40C′	1.74	163.2	141.8	47	random coil			
$^{1}J_{N,H}$						– 91.1	– 74.5	
$^{2}J_{N,O}$						8.6	8.2	
$^{3}J_{N,C'}$						– 0.6	– 0.9	0.3
F4^{H}N–S65C′	1.88	165.1	169.0	24	β-sheet			
$^{1}J_{N,H}$						– 100.3	-83.9	
$^{2}J_{N,O}$						6.7	7.0	
$^{3}J_{N,C'}$						– 0.8	– 1.0	0.56
K27^{H}N–I23C′[e]	2.02	169.9	152.8	141	α-helix			
$^{1}J_{N,H}$						– 88.0	– 70.8	
$^{2}J_{N,O}$						3.7	3.6	
$^{3}J_{N,C'}$						– 0.4	– 0.4	0.50
K33^{H}N–K29C′	2.03	156.8	143.5	99	α-helix			
$^{1}J_{N,H}$						– 88.2	– 70.9	
$^{2}J_{N,O}$						3.8	3.7	
$^{3}J_{N,C'}$						– 0.3	– 0.3	[f]
I23^{H}N–R54C′	1.92	155.8	175.7	47	random coil			
$^{1}J_{N,H}$						– 92.5	– 75.5	
$^{2}J_{N,O}$						5.4	5.7	
$^{3}J_{N,C'}$						– 0.8	– 0.9	0.50

[a] At the UHF or UB3LYP/6-31G(d,p) level. See footnotes [a] – [d] to Table 4. Geometries from ref. [19]. [b] OH distance in Å. [c] Approximate torsion angle between amide planes. [d] From ref. [7]. [e] Lysine side chain in protonated form (as in the experimental structure). For the neutral form, the corresponding values at same level are: $^{1}J_{N,H} = -71.3$, $^{2}J_{N,O} = 3.6$, $^{3}J_{N,C'} = -0.5$ Hz. [f] Not observed (< 0.25 Hz).

rather different according to the value of ϕ. Thus, for $\phi = 30^\circ$ (in a relatively strained arrangement, since the two molecules may be very close) most of the PES is repulsive, by 2 – 37 kcal mol^{-1}. Although such arrangements are obviously unlikely to be met in practice, it is of interest also to explore this part of the coupling surface in order to set an upper limit of these coupling constants. In fact, the strongest couplings (> 4 Hz) are expected for this arrangement. The interaction becomes weakly stabilizing only when $r > 2.0$ Å, $\psi > 150^\circ$. In this region, however, $^{3}J_{N,C'}$ reverts to "normal" values of about 1 Hz. The general trend is a decrease of J upon increasing r and ψ.

The PES for $\phi = 60 – 120^\circ$ are qualitatively similar to each other; there is no repulsive region, and the interaction becomes more stabilizing upon increasing r, with a small influence of ψ. For $\phi = 150^\circ$ the PES becomes repulsive at short ($r < 1.8$ Å) values, presumably for the same reasons seen for $\phi = 30^\circ$. The coupling surfaces show values ranging between 0.5 and 2 Hz, and show a noticeable dependence on ψ. Thus, $^{3}J_{N,C'}$ values go through a maximum at ψ about 150 – 160°, but the 1.5 Hz region (red region in Figure 3) is broader and almost independent of ψ if $\phi = 60^\circ$, while for $\phi =$ 90 – 150° the red region lies at $\psi > 150^\circ$. Hence, although large J values (ca. 2 Hz) are found for $\phi = 90^\circ$, $\psi = 180^\circ$ (i.e., a fully linear N–H ··· O=C group),[16] similar values are also found when the HB substantially deviates from linearity. Thus, J values between 1.8 – 2.0 Hz are also found for $\phi = 60 – 150^\circ$, provided that $r < 1.8$ Å and $\psi > 150^\circ$ (red regions in Figure 2). Therefore, a linear HB is not necessary to have strong couplings.

From an examination of Figure 3 it becomes apparent that, within the scope of the current model system, one can expect J couplings of the order of 0.5 – 1.5 Hz, the maximum values being reached for $r \approx 1.8$ Å and $\psi \approx 160^\circ$, where the HB interaction is still stabilizing. The picture is somewhat different for $\phi = 60^\circ$ (NHO angle 150°; the foremost surface in Figure 3), for which the dependence on ψ is much smaller and the values of J are larger on the average.

Having established that through-HB couplings can indeed be calculated for a model system in a reliable way (see also ref. [16]), the question remains of why such couplings should be observable at all. In fact, the three molecular orbitals of the formamide dimer depicted in Figure 4 which connect the two interacting molecules are probably responsible for the transmission of coupling; their σ symmetry (and especially the lack of π MOs with this property) is consistent with the scarce dependence of $^{3}J_{N,C'}$ on the torsion angle between the two amide planes discussed before. The connection between such observations and the bonding character of the HB (covalent or electrostatic), however, awaits further studies.[20]

Ubiquitin: Although the magnitudes are again overestimated, there is a good correlation (with one exception; see below) between calculated and experimental $^{3}J_{N,C'}$ values. The correlation is, however, of similar quality with both DFT and HF methods (Figure 5). In the case of K27–I23 the calculated couplings are much smaller than found. We investigated the possible effect of the state of ionization of the lysine side chain in K27 (i.e., whether as -NH_2 or -NH_3^+), but this is not relevant in determining the interresidue coupling, since we calculated identical values in both systems (Table 5). Given the good performance in all other cases, at present we cannot give an explanation in terms of errors in the calculations. It is possible that a) the actual conformation (and in particular the HB distance) of this part of the peptide molecule in solution is appreciably different from that in the solid state, or b) the experimental value should be revised (this appears much less probable, in view of the relatively large coupling constant observed). In either case, this problem highlights the fact that FC calculations are sensitive enough to furnish complementary data to experimental NMR measurements.

All experimental couplings fall within 0.3 – 0.8 Hz,[6–8] with hydrogen bonds having r between 1.8 – 2.0 Å and and NHO angle between 155 – 170° ($\phi = 65 - 80°$). From the model calculations one would expect $^3J_{N,C'} \approx 1$ Hz for such arrangements, which is consistent with the values found (when the overestimation is taken into account). Apparently, the failure to detect a coupling constant for K33–K29 stems not only from the longer HB distance ($r = 2.03$ Å), but from the value of $\psi = 143.5°$ as well, which place this system in a region where calculated couplings are indeed weak (0.5 – 0.7 Hz). In other words, there is a definite angular dependence of J coupling beyond the distance dependence. Accordingly, even though Bax et al.[8] could correlate the HB length with $^3J_{N,C'}$, the correlation showed considerable scatter (which was attributed to uncertainties in the X-ray structure, but may actually be due to the neglect of angular dependence). In fact, there is no well-defined correlation of $^3J_{N,C'}$ values[7] versus either r, ψ or ϕ, whereas (as judged from the few available data) the two-variable correlation of $^3J_{N,C'}$ versus (r,ψ) is somewhat better than with versus (r,ϕ) (data not shown).

Conclusion

The calculation of the Fermi-contact term appears to be a reliable method for the prediction and the understanding of through-HB couplings between amide groups. By making use of a relatively simple model system and peptide fragments in the appropriate orientation, one can make reasonable predictions of interresidue J couplings. It is then easy to foresee a rapid development of this area, for example a) improving the agreement with experimental values (this may require the inclusion of all other terms contributing to the coupling); b) further validating the reliability of these calculations in other cases. Eventually, the ability to establish the relationship between coupling constants and geometrical arrangement may provide a new type of constraint for molecular dynamics simulations, analogous to the NOE values that are now in common usage.

Computational Details

The Fermi-contact contribution to the scalar coupling constant between two nuclei M an N is calculated by FPT as in Equation (1):[5, 14, 21]

$$J_{M,N} = \left(\frac{\mu_0}{4\pi}\right)^2 \frac{\hbar}{2\pi}\left(\frac{8\pi\beta}{3}\right)^2 \frac{1}{a_0^6}\gamma_M\gamma_N\frac{1}{\lambda}B_{FC} \quad (1)$$

where μ_0 is the magnetic permeability of vacuum, β is the Bohr magneton, a_0 the Bohr radius, λ the applied perturbation (generally 10^{-3} au; the calculation is insensitive to the actual value[22]), γ_i the magnetogyric ratios of the involved nuclei, and B_{FC} the calculated Fermi-contact term in atomic units. The calculations were run with *Gaussian 98*[23] using spin-unrestricted HF or DFT (B3LYP)[23, 24] methods (selected through the *Field* keyword). Tight SCF convergence criteria were always employed, since the results were markedly different otherwise.

[1] a) G. A. Jeffrey, W. Saenger, *Hydrogen Bonding in Biological Structures*, Springer, Berlin, **1991**; b) J. Bernstein, M. C. Etter, L. Leiserowitz in *Structure Correlation* (Eds.: H.-B. Bürgi, J. D. Dunitz), VCH, Weinheim, **1994**.

[2] P. R. Blake, J. B. Park, M. W. W. Adams, M. F. Summers, *J. Am. Chem. Soc.* **1992**, *114*, 4931 – 4933.

[3] K. Pervushin, A. Ono, C. Fernández, T. Szyperski, M. Kainosho, K. Wüthrich, *Proc. Natl. Acad. Sci. USA* **1998**, *95*, 14147 – 14151.

[4] A. J. Dingley, S. Grzesiek, *J. Am. Chem. Soc.* **1998**, *120*, 8293 – 8297.

[5] A. J. Dingley, J. E. Masse, R. D. Peterson, M. Barfield, J. Feigon, S. Grzesiek, *J. Am. Chem. Soc.* **1999**, *121*, 6019 – 6027.

[6] F. Cordier, S. Grzesiek, *J. Am. Chem. Soc.* **1999**, *121*, 1601 – 1602.

[7] G. Cornilescu, J.-S. Hu, A. Bax, *J. Am. Chem. Soc.* **1999**, *121*, 2949 – 2950.

[8] G. Cornilescu, B. E. Ramirez, M. K. Frank, G. M. Clore, A. M. Gronenborn, A. Bax, *J. Am. Chem. Soc.* **1999**, *121*, 6275 – 6279.

[9] N. S. Golubev, I. G. Shenderovich, S. N. Smirnov, G. S. Denisov, H. H. Limbach, *Chem. Eur. J.* **1999**, *5*, 492 – 497.

[10] I. G. Shenderovich, S. Smirnov, G. S. Denisov, V, Gindin, N. S. Golubev, A. Dunger, R. Reibke, S. Kirpekar, O. L. Malkina, H. H. Limbach, *Ber. Bunsenges. Phys. Chem.* **1998**, *102*, 422 – 428.

[11] a) A. Bagno, G. Scorrano, S. Stiz, *J. Am. Chem. Soc.* **1997**, *119*, 2299 – 2300; b) A. Bagno, M. Campulla, M. Pirana, G. Scorrano, S. Stiz, *Chem. Eur. J.* **1999**, *5*, 1291 – 1300.

[12] A. Bagno, S. Gerard, J. Kevelam, E. Menna, G. Scorrano, *Chem. Eur. J.* **2000**, *6*, 2915 – 2924.

[13] T. Helgaker, M. Jaszuñski, K. Ruud, *Chem. Rev.* **1999**, *99*, 293 – 352.

[14] T. Onak, J. Jaballas, M. Barfield, *J. Am. Chem. Soc.* **1999**, *121*, 2850 – 2856.

[15] M. Pecul, J. Sadlej, *Chem. Phys. Lett.* **1999**, *308*, 486 – 494.

[16] C. Scheurer, R. Brüschweiler, *J. Am. Chem. Soc.* **1999**, *121*, 8661 – 8662.

[17] H. Adalsteinsson, A. H. Maulitz, T. C. Bruice, *J. Am. Chem. Soc.* **1996**, *118*, 7689 – 7693.

[18] F. B. van Duijneveldt in *Molecular Interactions* (Ed.: S. Scheiner), Wiley, Chichester, **1997**.

[19] S. Vijay-Kumar, C. E. Bugg, W. J. Cook, *J. Mol. Biol.* **1987**, *194*, 531 – 544. Ubiquitin from human erythrocytes (PDB file: 1UBQ).

[20] For a recent entry to this problem see: J. J. Dannenberg, L. Haskamp, A. Masunov, *J. Phys. Chem. A* **1999**, *103*, 7083 – 7086.

[21] D. P. Chong, S. R. Langhoff, C. W. Bauschlischer, *J. Chem. Phys.* **1991**, *94*, 3700 – 3706.

[22] V. G. Malkin, O. L. Malkina, D. R. Salahub, *Chem. Phys. Lett.* **1994**, *221*, 91 – 99.

[23] *Gaussian 98*, *Revision A.6*, M. J. Frisch, G. W. Trucks, H. B. Schlegel, G. E. Scuseria, M. A. Robb, J. R. Cheeseman, V. G. Zakrzewski, J. A. Montgomery, Jr., R. E. Stratmann, J. C. Burant, S. Dapprich, J. M. Millam, A. D. Daniels, K. N. Kudin, M. C. Strain, O. Farkas, J. Tomasi, V. Barone, M. Cossi, R. Cammi, B. Mennucci, C. Pomelli, C. Adamo, S. Clifford, J. Ochterski, G. A. Petersson, P. Y. Ayala, Q. Cui, K. Morokuma, D. K. Malick, A. D. Rabuck, K. Raghavachari, J. B. Foresman, J. Cioslowski, J. V. Ortiz, B. B. Stefanov, G. Liu, A. Liashenko, P. Piskorz, I. Komaromi, R. Gomperts, R. L. Martin, D. J. Fox, T. Keith, M. A. Al-Laham, C. Y. Peng, A. Nanayakkara, C. Gonzalez, M. Challacombe, P. M. W. Gill, B. Johnson, W. Chen, M. W. Wong, J. L. Andres, C. Gonzalez, M. Head-Gordon, E. S. Replogle and J. A. Pople, Gaussian, Inc., Pittsburgh PA, **1998**.

[24] A. D. Becke, *J. Chem. Phys.* **1993**, *98*, 5648.

Received: January 26, 2000 [F2262]

0947-6539/00/0616-2930 $ 17.50+.50/0